Automatic Ventral Intermediate Nucleus Localization Based on Anterior Commissure and Posterior Commissure

Riyanarto Sarno (riyanarto@if.its.ac.id)
Institut Teknologi Sepuluh Nopember Surabaya https://orcid.org/0000-0001-5373-660X
Kelly Rossa Sungkono
Institut Teknologi Sepuluh Nopember https://orcid.org/0000-0003-3030-3566
Mohammad Ardika Rifqi
Institut Teknologi Sepuluh Nopember
Achmad Fahmi
Universitas Airlangga
Agus Turchan
Universitas Airlangga
Abdul Hafid Bajamal
Universitas Airlangga

Research

Keywords: brain lesion, comparison experiment, magnetic resonance imaging, Parkinson's disease, ventral intermediate nucleus

Posted Date: October 20th, 2020

DOI: https://doi.org/10.21203/rs.3.rs-19214/v2

Automatic Ventral Intermediate Nucleus Localization Based on Anterior Commissure and Posterior Commissure

Riyanarto Sarno[1]* • Kelly Rossa Sungkono[1] • Mohammad Ardika Rifqi[1]
Achmad Fahmi[2,3] • Agus Turchan[2,3] Abdul Hafid Bajamal[2,3]

*Corresponding author's Email: riyanarto@if.its.ac.id
[1]Department of Informatics, Institut Teknologi Sepuluh Nopember Surabaya, Indonesia
[2]Department of Neurosurgery, Faculty of Medicine, Airlangga University, Indonesia
[3]Dr. Soetomo General Academic Hospital, Medical Center. Indonesia

Abstract

The ventral intermediate nucleus (Vim), as the motor thalamic nuclei section, is a generally used target in brain lesion surgery or stimulation for decreasing tremors in people with Parkinson's disease. Determining the exact position of Vim is challenging because Vim cannot be visualized clearly in commonly used magnetic resonance imaging (MR). Indirect methods, i.e., Coordinate-based targeting and Guiot's, utilize anterior commissure and posterior commissure to detect the location of Vim. In practice, neurosurgeons manually implement these methods in existing neurosurgical planning software, so the accuracy of the targeting depends on their memory and foresight. Afterward, Coordinate-based targeting and Guiot's locate Vim based on anterior commissure (AC) and posterior commissure (PC), so neurosurgeons must correctly determine AC and PC. This paper proposes automatic indirect methods and measures the accuracy of indirect methods in MRIs with correct and incorrect orientations of AC-PC planes. An objective of analyzing indirect methods in MRIs with incorrect orientations of AC-PC planes is to discover the most resilient indirect method with inaccuracy AC-PC planes. To develop automatic indirect methods, the first step is redefining the plane passing through three defined points, i.e., AC, PC, and midline reference, by a quaternion. Secondly, Coordinate-based targeting and Guiot's are implemented to determine the Vim targeting location automatically. This paper converts the rules of those methods in voxels because the rules use millimeters while the three-dimensional MRIs use voxels. The experiment shows that Vim locations obtained by Guiot's are more accurate than those by Coordinate-based targeting in MRIs with the correct orientation of AC-PC planes. Guiot's has 0.05 mm smaller value of average error results than Coordinate-based targeting. In contrast, Vim locations based on Coordinate-based targeting are more accurate in the MRIs with the incorrect orientation of AC-PC planes. Coordinate-based targeting has 0.032 mm smaller value of average error results than Guiot's.

Keywords: brain lesion, comparison experiment, magnetic resonance imaging, Parkinson's disease, ventral intermediate nucleus.

1. INTRODUCTION

Parkinson's disease (PD) has the fastest enhancement worldwide among neurological disorders. The number of affected individuals in 2016 was more than doubled times as high as individuals in 1990 [1]. Southeast Asia contributed six portions of overall affected individuals, and Indonesia is the largest contributor in Southeast Asia. Nevertheless, there is no treatments or medicines which cure PD [2, 3]. Current treatments of PD focus on reducing its symptoms; one of them is tremor.

There are some treatments to decrease Parkinson's disease, such as drug administration [4, 5], brain lesion [2, 6, 7], and deep brain stimulation [8–10]. A common brain part as the target of deep brain stimulation and brain lesion is ventral intermediate nucleus (Vim) [9]. Vim is a section of Thalamic nuclei, and it has been anatomic target treatments for movement disorders, including PD [11].

Although Vim is designated as a target of PD treatments, determining the exact position of Vim is challenging. Vim locations cannot be visualized clearly in 3 Tesla magnetic resonance imaging (MR) [3, 12]. By looking at the difficulty of detecting the location of the Vim, some indirect methods are developed. The widely used indirect methods are Coordinate-based targeting [2, 13] and Guiot's [14, 15].

Coordinate-based targeting determines the coordinates of the Vim based on the human brain atlas data, i.e. Schatelbrand-Bailey's atlas [16]. Coordinate-based targeting defines Vim location is 15 mm x-coordinate from AC-PC line and around 6 mm y-coordinate from posterior commissure (PC). AC point is a center point in the border of AC and PC point is a center point in the border of PC. Guiot's method [17, 18] determines the y-coordinate of the Vim based on the real distance between the anterior commissure (AC) and the posterior commissure (PC) of the patient and the x-coordinate based on the Coordinate-based targeting method. Guiot's defines one-fourth or three-twelfth of AC-PC line as the y-coordinate of the Vim. Successful determination of Vim based on these indirect methods depends on the accuracy of AC and PC.

To facilitate Vim locations determination, neurosurgical planning applications are available, i.e. Leksell Surgiplan [17–19] and Inomed Planning Software (IPS) [20]. Both of those applications provide displaying three-dimensional views of an MRI and measuring the distance between brain parts. Except for those capabilities, all neurosurgical planning applications have no feature of automatic indirect methods. Neurosurgeons need their memory and their ability to implement indirect methods in those applications.

Referring to previous explanation, there were several motivations to form this study:

a. Development of automatic indirect methods has not been excavated by existing neurosurgical planning applications, provides open opportunities for contribution. A challenge that must be faced in developing automatic indirect methods is the difference between a used scale of indirect methods and a scale of MRI. Coordinate-based targeting and Guiot's establish their rules in millimeter-scale; however, MRIs are recorded in voxel-scale.
b. Coordinate-based targeting and Guiot's determine left and right Vim locations based on AC-PC plane. AC-PC planes are determined based on AC-PC points. If the AC-PC points are not aligned accurately, then AC-PC planes are not correct. Existing studies focus on the accuracy in MRIs with correct orientation of AC-PC planes or the impact of indirect methods to people with PD [2, 3, 21, 22]. No study analyzes indirect methods in MRIs with the incorrect orientation of AC-PC planes.

Based on those motivations, this paper proposes automatic indirect methods of Vim localizations. It analyzes indirect methods in cases of MRIs with the correct and incorrect orientation of AC-PC planes. There are several steps for developing proposed automatic indirect methods. First, the brain MRIs are aligned automatically based on defined AC point, a PC point, and a midline reference (MR) line. Then, the proposed automatic indirect methods convert the coordinates from millimeters to voxels to determine the Vim location. The conversion is applied because rules of Coordinate-based targeting and Guiot's uses millimeters while three-dimensional MRIs are measured in voxels. The Vim locations obtained by proposed automatic indirect methods are compared with those determined manually by neurosurgeons.

This paper analyzes indirect methods by measuring the accuracy of Coordinate-based targeting and Guiot's based on MRIs with correct and incorrect orientation of AC-PC planes. This paper uses thirty post-operative 3T T2-Flair MRIs in the experiment. In MRIs with the correct orientation of AC-PC planes, Vim locations based on those two methods are compared with ground truth. The ground truth in this paper is a set of centers of Vim brain lesions which are captured in post-operative T2-Flair MRIs. Thereupon, in MRIs with incorrect orientation of AC-PC planes, each Vim location obtained by one of those methods from MRI with incorrect orientation is compared with its obtained by same method from MRI with the correct orientation. MRIs with the incorrect orientation are formed by rotating with specific degrees on x-axis rotation, y-axis rotation, and z-axis rotation. Euclidean distance is used to determine the accuracy, wherein smaller Euclidean distance means higher accuracy of Vim locations determination.

The remainder of this paper is structured as follows: Section 2 explains parts of the brain which are utilized in determining Vim locations, indirect methods, and the measurement methods. Section 3 describes the proposed automatic indirect methods. Section 4 provides the experiment results and analysis related to the obtained results. The last section, Conclusion section, sums up all works of this study.

2. RELATED METHODS

2.1. Ventral Intermediate Nucleus

The ventral intermediate nucleus (Vim) is commonly used in the surgical treatment of Parkinsonian and essential tremors [23]. The Vim is a nuclear part of the thalamus, which delivers signals from sensors, such as motor signals. The location of the Vim cannot be identified with certainty by using commonly magnetic resonance imaging. However, it can be detected by referring to surrounding parts of a brain. The center point of Vim is located approximately 1.5 mm next to the corticospinal tract (CST), which can be observed clearly in MRIs with T2-fluid-attenuated inversion recovery (T2-FLAIR) sequences. Referring to Figure 1, left and right CSTs are white areas in red circles while left and right Vims are located in the yellow circles.

.

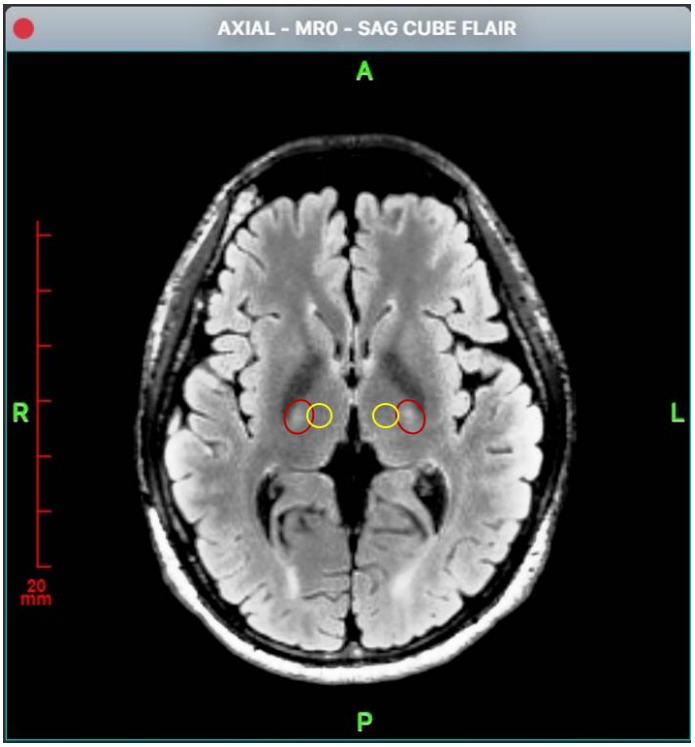

Figure 1. Axial plane in 3T brain magnetic resonance imaging (MRI)

2.2. Anterior Commissure, Posterior Commissure and Midline Reference

The anterior commissure (AC), posterior commissure (PC), and midline (mid-sagittal plane) reference (MR) are used to align the brain [24]. The location of the AC is in the anterior wall of the third ventricle at the upper end of the lamina terminals. The area of the PC is in the posterior wall of the third ventricle. The anterior commissure – posterior commissure line (AC-PC line), defined by Talairach [25], is a line that connects an AC point (a center point in the border of AC) and a PC point (a center point in the border of PC). AC-PC points can be determined based on the sagittal plane and the axial plane. AC-PC points are symbolized as green signs, and an AC-PC line is visualized as a yellow line of Figure 2.

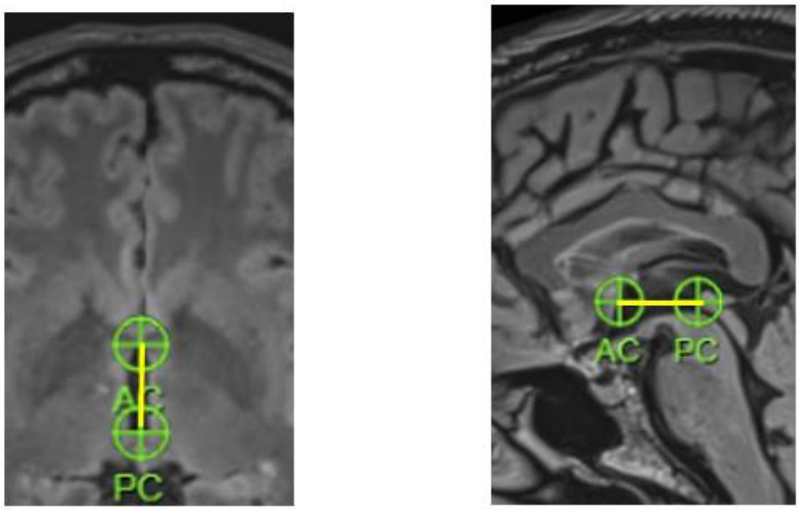

(a) Axial plane **(b) Sagittal plane**

Figure 2.AC-PC in the axial plane and the sagittal plane

After determining the points of AC-PC, the midline (mid-sagittal plane) reference (MR) is determined. The mid-sagittal plane divides the left and the right brain. The point of MR is obtained based on a point in a line that is perpendicular to the AC-PC line and splits the brain stem. MR is denoted as M2 (the yellow circle) in Figure 3.

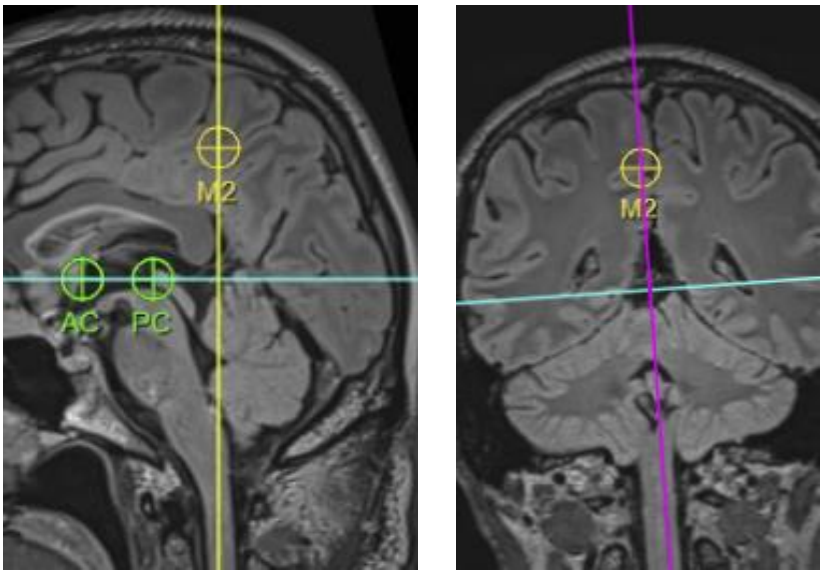

(b) Sagittal plane **(b) Coronal plane**

Figure 3. MR in the sagittal plane and the coronal plane

2.3. Indirect Methods for Determining Vim Localization

There are two general indirect methods for finding the location of Vim, i.e. Coordinate-based targeting and Guiot's method. Coordinate-based targeting [2, 13] is a Vim localization method based on the human brain atlas data, i.e. Schatelbrand-Bailey's atlas. The equations for locating the Vim are given in Theorem 1, whose symbols are explained in Definition 1. Red circles of Figure 2 represent right and left Vim obtained by Coordinate-based targeting. M4 and M3 denote a right posterior endpoint of the globus pallidus and a left posterior endpoint of the globus pallidus. M5 is a center of a brain lesion which is used as the ground truth in the experiment.

Definition 1. *AC* is the point of the anterior commissure and *PC* is the point of the posterior commissure in the anterior commissure-posterior commissure plane; (x_{AC}, y_{AC}) are the *x*-coordinate and the *y*-coordinate of the anterior commissure; (x_{PC}, y_{PC}) are the *x*-coordinate and the *y*-coordinate of the posterior commissure; $(x_{VIM_{M_R}}, y_{VIM_{M_R}})$ are the *x*-coordinate and the *y*-coordinate of the right Vim in the MRI based on the method; $(x_{VIM_{M_L}}, y_{VIM_{M_L}})$ are the *x*-coordinate and the *y*-coordinate of the left Vim in MRI based on the method; $d(AC, PC)$ is the distance between the anterior commissure (AC) and the posterior commissure (PC).

Theorems 1.

$(x_{VIM_{M_R}}, y_{VIM_{M_R}}) = (x_{PC} - 15mm, y_{PC} + [6,7] \times d(AC, PC))$ and $(x_{VIM_{M_R}}, y_{VIM_{M_R}}) = (x_{PC} + 15mm, y_{PC} + [6,7] \times d(AC, PC))$

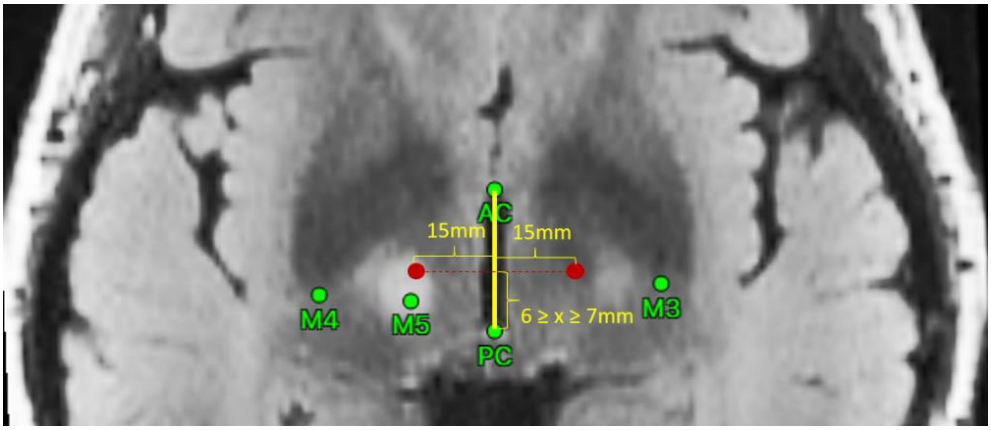

Figure 4. Coordinate-based targeting method

Guiot's method [14, 15] determines the y-coordinate of the Vim based on the real distance between AC and PC of the patient and the x-coordinate based on the Coordinate-based targeting method. The equations for locating the Vim are given in Theorem 2, whose symbols are explained in Definition 1. The red circles of Figure 5 represent right and left Vim obtained by Guiot's.

Theorem 2.

$$(x_{VIM_{M_R}}, y_{VIM_{M_R}}) = \left(x_{PC} - 15mm, y_{PC} + \frac{1}{4} d(AC, PC) mm \right) \text{and } \left(x_{VIM_{M_L}}, y_{VIM_{M_L}} \right) = \left(x_{PC} + 15mm, y_{PC} + \frac{1}{4} d(AC, PC) mm \right)$$

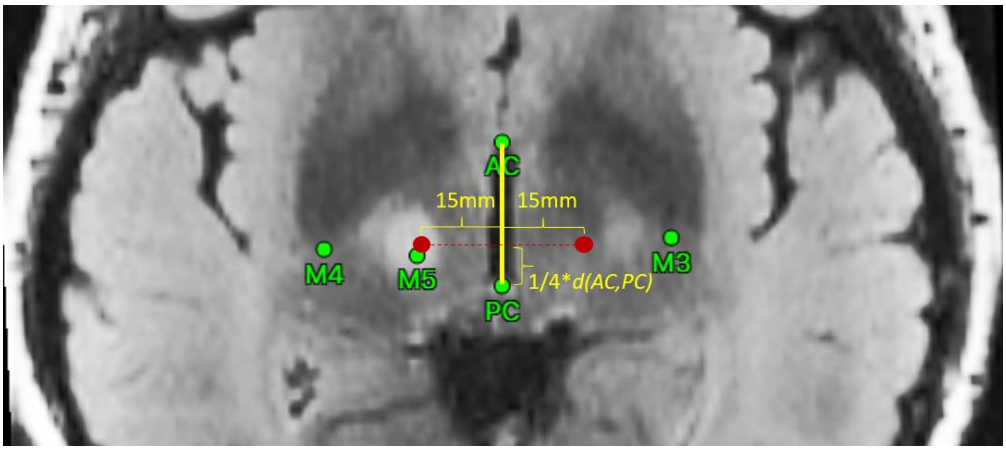

Figure 5. Guiot's method

2.4. Measurements of Accuracy

This paper measures the accuracy of Coordinate-based targeting and Guiot's based on MRIs with the correct and incorrect orientation of AC-PC planes. In MRIs with the correct orientation of AC-PC planes, Vim locations based on those two methods are compared with ground truth. The ground truth in this paper is a set of centers of dark spots in Vim brain lesions which are captured in post-operative T2-Flair MRIs. Thereupon, in MRIs with incorrect orientation of AC-PC planes, each Vim location obtained by one of those methods from MRI with the incorrect orientation is compared with its obtained by same method from MRI with correct orientation. MRIs with the incorrect orientation are formed by rotating with specific degrees on x-axis rotation, y-axis rotation, and z-axis rotation. The illustration of x-axis, y-axis and z-axis is shown in Figure 6. The specific degrees in this experiment are $-10^{\circ}, -5^{\circ}, 5^{\circ}, 10^{\circ}$ x-axis rotations, $-10^{\circ}, -5^{\circ}, 5^{\circ}, 10^{\circ}$ y-axis rotations, and $-10^{\circ}, -5^{\circ}, 5^{\circ}, 10^{\circ}$ z-axis rotations.

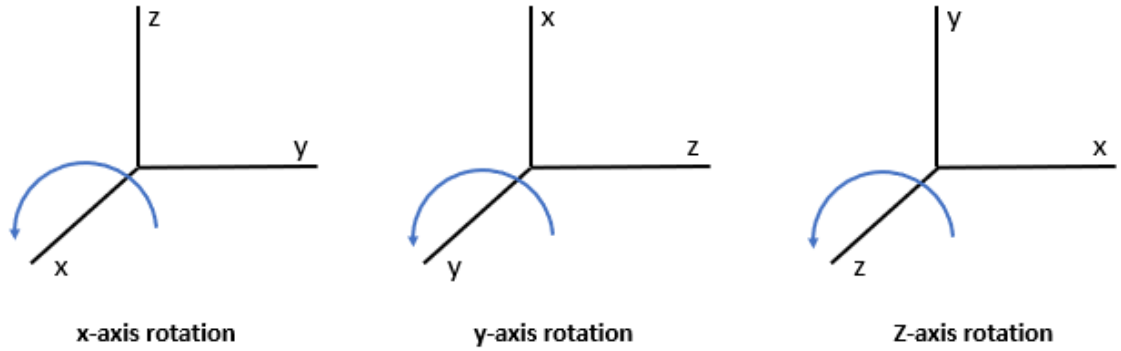

Figure 6. 3D Axis Rotation

This paper determines accuracy based on error results. Error results are obtained based on Euclidean distance of reference points and Vim locations based on indirect methods (Coordinate-based targeting and Guiot's). In MRIs with correct orientation of AC-PC planes, error results are calculated for each patient. On the other hand, in MRIs with incorrect orientation of AC-PC planes, error results of all patients are averaged for each degree of each axis rotation (x-axis, y-axis, or z-axis). The method gains high accuracy if the average error result is small, and vice versa. Error results based on MRIs with correct and incorrect orientation of AC-PC planes are determined in Equation (1) and Equation (2).

$$ER_n = \sqrt{\left(x_{G_n} - x_{M_n}\right)^2 + \left(y_{G_n} - y_{M_n}\right)^2 + \left(z_{G_n} - z_{M_n}\right)^2} \tag{1}$$

where: ER_n : error result of each patient in a medical image (MRI) with correct orientation of AC-PC planes
n : number of patients
x_{M_n} : x-coordinate of Vim location determined by a Vim targeting method
x_{G_n} : x-coordinate of a center of a dark spot in a Vim brain lesion as ground truth
y_{M_n} : y-coordinate of Vim location determined by a Vim targeting method
y_{G_n} : y-coordinate of a center of a dark spot in a Vim brain lesion as ground truth
z_{M_n} : z-coordinate of Vim location determined by a Vim targeting method
z_{G_n} : z-coordinate of a center of a dark spot in a Vim brain lesion as ground truth

$$AER_D = \frac{\sum_1^n \sqrt{\left(x_{M_{D_n}} - x_{M_{0_n}}\right)^2 + \left(y_{M_{D_n}} - y_{M_{0_n}}\right)^2 + \left(z_{M_{D_n}} - z_{M_{0_n}}\right)^2}}{n} \tag{2}$$

where: AER_D : average error results in medical images with a certain degree of a certain axis (x-axis, y-axis, or z-axis)
n : number of patients
D : degree of certain axis
$x_{M_{D_n}}$: x-coordinate of Vim location determined by a Vim targeting method in a medical image with a certain degree of a certain axis
$x_{M_{0_n}}$: x-coordinate of Vim location determined by a Vim targeting method in a medical image with 0° degree toward x, y, and z planes
$y_{M_{S_n}}$: y-coordinate of Vim location determined by a Vim targeting method in a medical image with a certain degree of a certain axis
$y_{M_{0_n}}$: y-coordinate of Vim location determined by a Vim targeting method in a medical image with 0° degree toward x, y, and z planes

$z_{M_{S_n}}$: z-coordinate of Vim location determined by a Vim targeting method in a medical image with a certain degree of a certain axis

$z_{M_{0_n}}$: z-coordinate of Vim location determined by a Vim targeting method in a medical image with 0° degree toward x, y, and z planes

3. MATERIAL AND METHODS

3.1. Material

This paper used thirty post-operative magnetic resonance imaging 3 Tesla (MRI 3T) of people with PD. These MRI 3T modalities are from T2-fluid-attenuated inversion recovery (T2-FLAIR) sequences. There are some reasons of using post-operative MRI 3T with T2-Flair sequences. First, MRIs with T2-Flair define clearly anatomical landmarks, namely AC and PC, to support Vim determination [22]. Secondly, post-operative MRIs are chosen because they visualized brain lesions. Centers of darker spots in brain lesions are appointed as ground truth in this paper. M5 point of Figure 7 indicates the center and white areas surrounding M5 are a brain lesion.

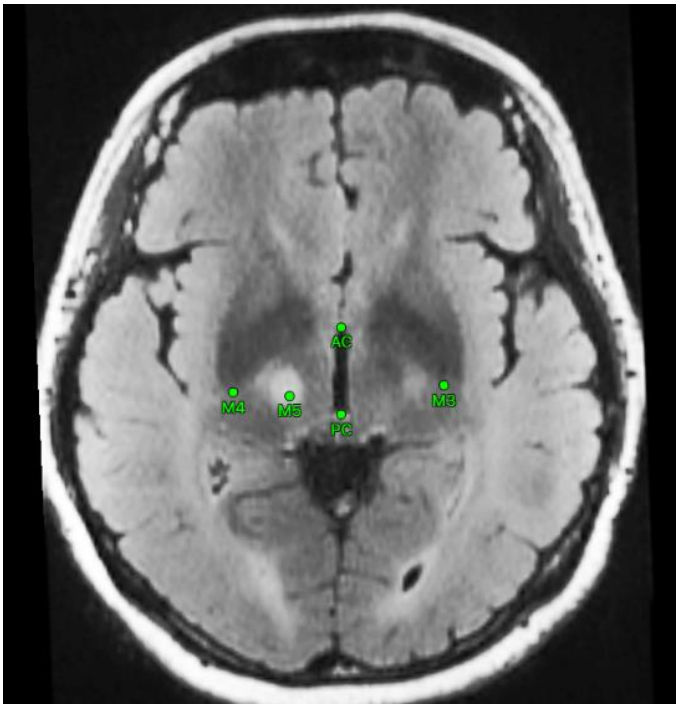

Figure 7. Axial plane of post-operative T2-Flair Brain MRI

Out of thirty patients, 72% are men with PD. Parkinson's disease affects more men; statistics in 2016 expose a ratio of men and women with PD is 1.7:1.2 [1]. The other information of patients whose data were used in the experiment is shown in Table 1. The length of AC-PC line has an average of 23.766 [1.513] mm. The high standard deviation scores of AC and PC point indicate the high difference in location of AC and PC point. The high difference of location of those points manifests differences in brain morphology of one patient and others.

Table 1. Details of Patients (people with PD)

	Mean (mm)	Standard Deviation (mm)
Anterior Commissure (AC) Point		
x-coordinate	77.932	6.556
y-coordinate	127.181	8.286
z-coordinate	141.133	6.115
Posterior Commissure (PC) Point		
x-coordinate	77.787	6.755

y-coordinate	103.929	8.505
z-coordinate	137.038	6.236
Length of AC-PC Line	23.766	1.513

3.2. Methods

This paper develops automatic indirect methods to determine Vim location. There are three steps in developed methods: (1) defining the anterior commissure (AC), posterior commissure (PC) and midline reference (MR) points in 3-vector coordinates; (2) redefining the plane passing through those points using 3 normal vectors which have been rotated by a quaternion; and (3) determining the Vim targeting location based on Coordinate-based targeting and Guiot's method.

3.2.1. Defining Anterior Commissure, Posterior Commissure and Midline Reference

Anterior commissure (AC) point, posterior commissure (PC), and midline (mid-sagittal plane) reference (MR) are used to align the brain [24]. Those points and midline are manually determined by neurosurgeons. The brain alignment based on defined points and midline is performed automatically in our developed methods.

Based on the points of AC, PC, and MR, the plane for determining the Vim location is obtained (denoted as Plane A or Pa). A visualization of Pa is shown in Figure 8. The position of this plane is in the center of the brain. C in Figure 9 is the center point of the plane. Even though Pa has been obtained, the geometric calculation cannot be conducted on the plane; this paper redefines Pa using 3 normal vectors which have been rotated by a quaternion [26, 27].

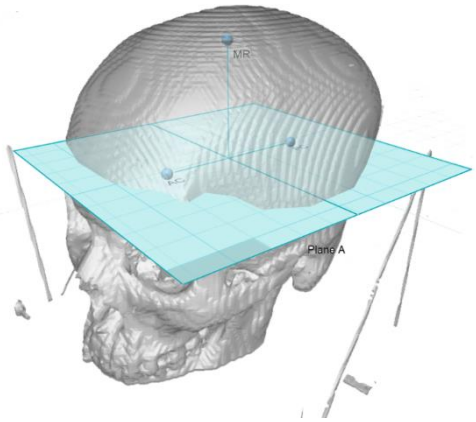

Figure 8. Visualization of a plane that is inside a head

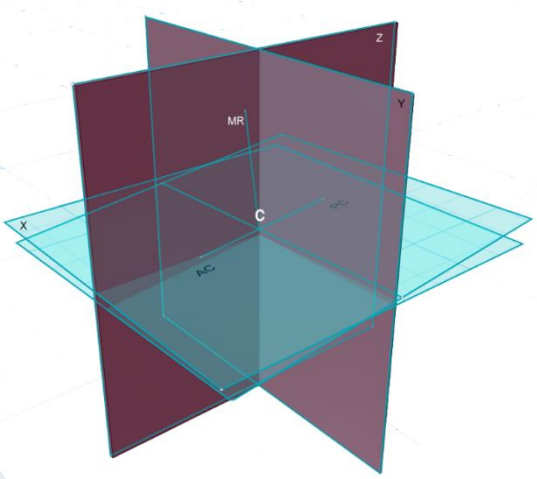

Figure 9. The position of Plane A between normal x-plane, y-plane, and z-plane.

3.2.2. Redefining The plane

The redefinition of the plane is explained step by step in Algorithm 1. The inputs are the points of AC, PC, MR and 3 normal vectors. The result is 3 normal vectors which have been rotated by a quaternion [26].

Algorithm 1: Redefine The Obtained Plane

Inputs: AC, PC, MR and 3 normal vectors which are determined by Equation (3)

Outputs: $\overrightarrow{Nr_x}$, $\overrightarrow{Nr_y}$, $\overrightarrow{Nr_z}$

1. Calculate the quaternion $Q1$ between $\overrightarrow{Nr_y}$, and $\overrightarrow{ACPC}$ based on Equations (4) and (5)
2. Project AC (T'_{AC}) and MR (T'_{MR}) to Py based on Equations (6) to (13) [26]
3. Calculate the angle of T'_{AC} and T'_{MR}, then multiply it by $Q1$ based on Equations (14) and (15) [26]
4. Rotate the normal vector using $Q1$ based on Equations (16) and (18)

$$\overrightarrow{N_x} = \begin{bmatrix}1\\0\\0\end{bmatrix}, \qquad \overrightarrow{N_y} = \begin{bmatrix}0\\1\\0\end{bmatrix}, \qquad \overrightarrow{N_z} = \begin{bmatrix}0\\0\\1\end{bmatrix} \tag{3}$$

$$\overrightarrow{ACPC_N} = \frac{\overrightarrow{ACPC}}{\sqrt{(AC_x - PC_x)^2 + (AC_y - PC_y)^2 + (AC_z - PC_z)^2}} \tag{4}$$

$$Q1 = QuatFromTwoVector(\overrightarrow{N_y}, \overrightarrow{ACPC_N}) \tag{5}$$

$$QProject = QuatMul\left(Q1, QuaternionFromAxisAngle\left(\overrightarrow{N_x}, -90^0\right)\right) \tag{6}$$

$$QProject = QuatMul\left(QProject, QuaternionFromAxisAngle\left(\overrightarrow{N_z}, 180^0\right)\right) \tag{7}$$

$$QProject = \begin{bmatrix}-QProject_x\\-QProject_y\\-QProject_z\\QProject_w\end{bmatrix} \tag{8}$$

$$ProjectMatrix = QuatToMatrix3x3(QProject) \tag{9}$$

$$T_{AC} = AC - C \tag{10}$$

$$T_{MR} = MR - C \tag{11}$$

$$T'_{AC} = T'_{AC} \times ProjectMatrix \tag{12}$$

$$T'_{MR} = T'_{MR} \times ProjectMatrix \tag{13}$$

$$T_{angle} = \text{atan}\left(\frac{T'_{AC_x} - T'_{MR_x}}{T'_{AC_y} - T'_{MR_y}}\right) \tag{14}$$

$$Q1 = QuatMul\left(Q1, QuaternionFromAxisAngle\left(\overrightarrow{N_y}, -T_{angle}\right)\right) \tag{15}$$

$$\overrightarrow{Nr_x} = QuatRotateVector(Q1, \overrightarrow{N_x}) \tag{16}$$

$$\overrightarrow{Nr_y} = QuatRotateVector(Q1, \overrightarrow{N_y}) \tag{17}$$

$$\overrightarrow{Nr_z} = QuatRotateVector(Q1, \overrightarrow{N_z}) \tag{18}$$

where: $\overrightarrow{N_x}$: normal vector of x plane
$\overrightarrow{N_y}$: normal vector of y plane
$\overrightarrow{N_z}$: normal vector of z plane
$\overrightarrow{ACPC}$: previous vector of AC-PC
$\overrightarrow{ACPC_N}$: vector of AC-PC after normalized
$Q1$: quaternion between $\overrightarrow{N_y}$ and $\overrightarrow{ACPC}$

$QProject_x$: rotation of x-axis of a rotation matrix denoted as $QProject$
$QProject_y$: rotation of y-axis of a rotation matrix denoted as $QProject$
$QProject_z$: rotation of z-axis of a rotation matrix denoted as $QProject$
$QProject_w$: *acos* of the rotation angle of a rotation matrix denoted as $QProject$
$ProjectMatrix$: left-handed 3x3 rotation matrix of $QProject$
AC : point of anterior commissure
MR : midline reference
C : point of center
T'_{AC} : project anterior commissure (AC)
T'_{MR} : project midline reference (MR)
T_{angle} : angle of T'_{AC} and T'_{MR}
$\overrightarrow{Nr_x}$: rotated normal vector of x plane
$\overrightarrow{Nr_y}$: rotated normal vector of y plane
$\overrightarrow{Nr_z}$: rotated normal vector of z plane

3.2.3. Determining Vim Location

The last step is determining the Vim location. The automatic Vim localization based on Guiot's method is determined by Equations (19) to (21), while that based on Coordinate-based targeting is determined by Equations (22), (23), and (21).

$$distFromPC = \frac{1}{4} \times \frac{\overrightarrow{ACPC}}{\sqrt{(AC_x - PC_x)^2 + (AC_y - PC_y)^2 + (AC_z - PC_z)^2}} \tag{19}$$

$$P = PC + \left(distFromPC \times \overrightarrow{ACPC}\right) \tag{20}$$

$$VIM = P \pm \frac{15}{VoxelSpacing \times \overrightarrow{Nr_x}} \tag{21}$$

$$distFromPC = rand(6,7) \tag{22}$$

$$P = PC + \left(\frac{distFromPC}{VoxelSpacing \times \overrightarrow{Nr_x}}\right) \tag{23}$$

where: $distFromPC$: distance of PC point and Vim point in the x-plane
$VoxelSpacing$: amount of space between voxels in the 3D medical images
PC : point of posterior commissure (PC)

4. RESULTS AND ANALYSIS

In this section, our proposed automatic indirect methods are evaluated by comparing the Vim locations obtained by our methods with those obtained by manual determination by a neurosurgeon on post-operative MRIs. Subsequently, Vim locations based on Coordinate-based targeting methods and those based on Guiot's are compared based on MRIs with correct orientation of AC-PC planes and MRIs with incorrect orientation of AC-PC planes.

4.1. Evaluation of Proposed Automatic Indirect Methods

Vim locations on 3-planes based on our proposed automatic indirect methods and those based on manual determination by a neurosurgeon are shown in Figure 10. The proposed automatic indirect methods were implemented with Node.js [28]. A neurosurgeon determines Vim locations manually by an existing neurosurgical planning application, which is IPS. Based on Figure 10, the positions of Vim by automatic indirect methods and manual indirect methods are similar. It can be concluded that our proposed indirect methods obtain correct locations of Vim.

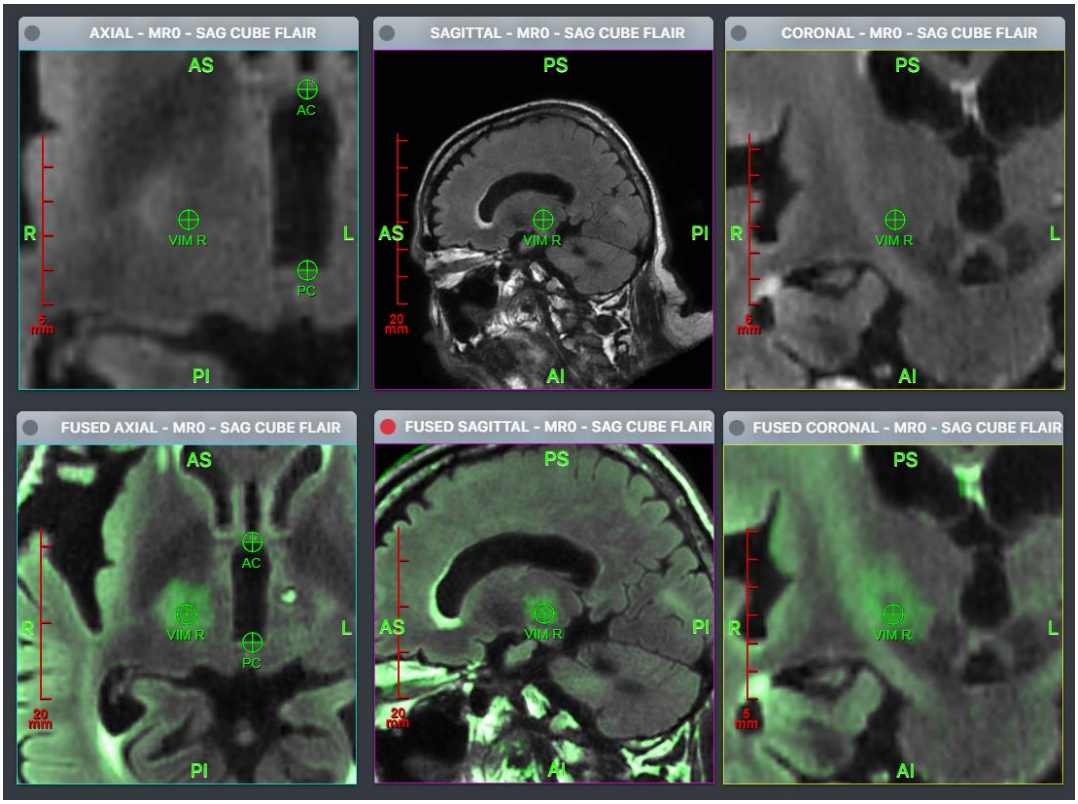

Figure 10. Comparison between the proposed method (above) and the manual determination of a neurosurgeon (below).

4.2. Evaluation of Indirect Methods in MRIs with Correct Orientation of AC-PC planes and MRIs with Incorrect Orientation of AC-PC planes

Indirect methods, i.e., Guiot's and Coordinate-based targeting, are compared based on correct and incorrect orientation of AC-PC planes. Correct orientation of AC-PC planes means used MRIs are already aligned based on AC, PC, and MR. Incorrect orientation of AC-PC planes means MRIs with correct orientation are rotated with specific degrees on x-axis, y-axis and z-axis. The specific degrees in this experiment are $-10^{\circ}, -5^{\circ}, 5^{\circ}, 10^{\circ}$.

Table 2 shows the average error results based on MRIs with the correct orientation of AC-PC planes. The average results of all patients show Coordinate-based targeting has 0.05 mm higher value of average error results of all patients than Guiot's. Briefly, Vim locations obtained by Guiot's is more accurate than those obtained by Coordinate-based targeting.

By analyzing results in Table 2, there are several data with >1.5 mm errors. There are some underlying causes. First, a person with PD, denoted by 6^{th} patient, has unusual brain morphology because of a cyst that affected corpus callosum. The comparison of a patient with a cyst and a patient without a cyst is shown in Figure 11. Red circles denote two corpus callosum. The corpus callosum that is pressed by the cyst is smaller than a normal corpus callosum. Shrinking corpus callosum causes shrinking of AC-PC line. Shrinking of AC-PC line raises errors in determining Vim locations. Secondly, the experiment of this paper used post-operative MRIs. Post-operative MRIs have differences with pre-operative MRIs. However, indirect methods are destined to a planning stage, so implementing those methods in post-operative MRIs reduces the accuracy of those methods.

Table 3 shows the average error results based on MRIs with the incorrect orientation of AC-PC planes. The average results of all rotations show Coordinate-based targeting has 0.032 mm smaller value of average error results of all rotations than Guiot's. It can be concluded that Vim locations based on Coordinate-based targeting are more accurate in MRIs with the incorrect orientation of AC-PC planes. Therefore, Coordinate-based targeting is more resilient with inaccuracy AC-PC planes.

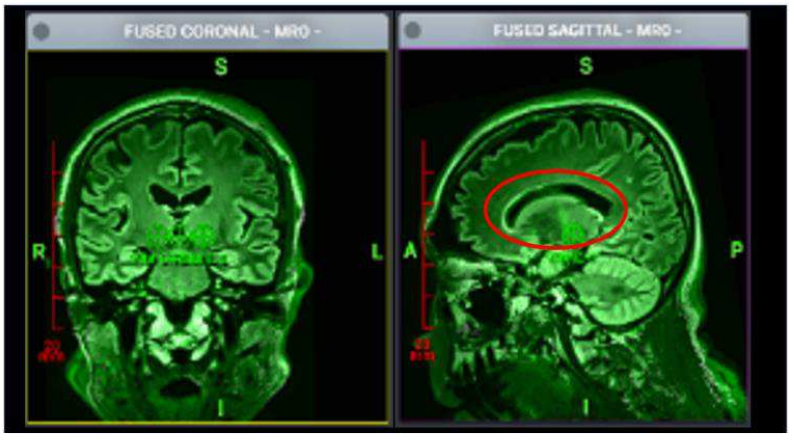

(a) Coronal and Axial Planes of a person with Parkinson's Disease without Having Cyst

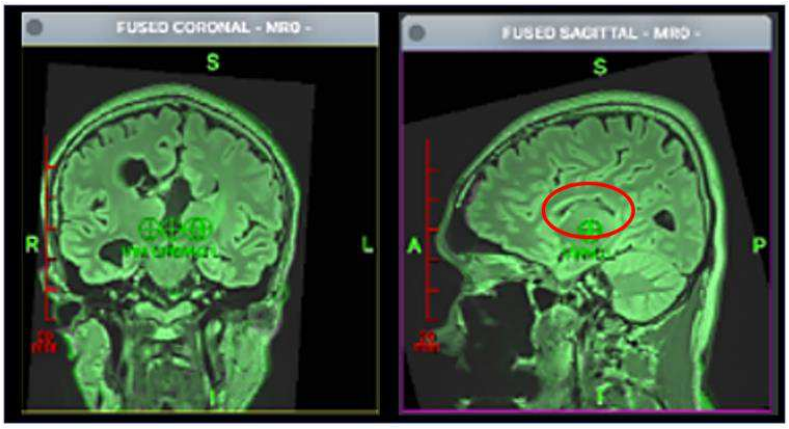

(b) Coronal and Axial Planes of a person with Parkinson's Disease with Having Cyst

Figure 11. Comparison of MRIs with and without Cyst

Table 2. Average Error Results based on MRIs with Correct Orientation of AC-PC Planes

Average of Error Results (mm)		**Indirect Methods**	
		Guiot's	**Coordinate-based targeting**
Average of Error Results based on Distance (Euclidean)	1st Patient	0.26	0.25
	2nd Patient	0.16	0.16
	3rd Patient	3.08	3.18
	4th Patient	1.24	1.16
	5th Patient	2.92	3.11
	6th Patient	4.37	4.22
	7th Patient	3.62	3.28
	8th Patient	3.09	3.55
	9th Patient	3.62	3.61
	10th Patient	0.59	0.70
	11th Patient	0.50	0.38
	12th Patient	1.62	1.85
	13th Patient	22.21	22.38
	14th Patient	2.05	3.01
	15th Patient	6.38	5.98
	16th Patient	3.58	3.99
	17th Patient	0.54	0.55

18th Patient	6.85	6.58
19th Patient	1.35	1.36
20th Patient	0.43	0.54
21st Patient	1.62	1.64
22nd Patient	3.38	2.85
23rd Patient	0.64	0.39
24th Patient	1.96	1.12
25th Patient	1.03	1.33
26th Patient	1.82	2.83
27th Patient	4.34	4.13
28th Patient	2.27	2.46
29th Patient	4.40	4.25
30th Patient	1.03	1.46
Average Results of All Patients	**3.03**	**3.08**

Table 3. Average of Error Results based on MRIs with Incorrect Orientation of AC-PC Planes

Average of Error Results based on Euclidean Distance (mm)		**Guiot's**	**Coordinate-based targeting**
X-Axis Rotation (degree)	-10	1.076	0.979
	-5	0.539	0.490
	5	0.539	0.491
	10	1.076	0.979
Y-Axis Rotation (degree)	-10	2.722	2.722
	-5	1.361	1.362
	5	1.380	1.380
	10	2.750	2.751
Z-Axis Rotation (degree)	-10	2.924	2.888
	-5	1.481	1.461
	5	1.487	1.475
	10	2.931	2.903
Average Results of all rotations		**1.689**	**1.657**

5. CONCLUSION

This paper develops proposed automatic indirect methods of VIM localization and observes Vim locations based on indirect methods in MRIs with the correct orientation of AC-PC planes and MRIs with the incorrect orientation of AC-PC planes. There are several steps of automatic indirect methods. The first step is determining the plane of the anterior commissure (AC) and the posterior commissure (PC) because this paper presents the center of the MRI image as the middle point of the AC-PC plane. The methods are automatically determining the AC-PC plane based on defined an AC point, a PC point, and a midline reference (MR) line. Then, the proposed automatic methods convert the coordinates from millimeters to voxels to determine the Vim location. The conversion is applied because rules of Coordinate-based targeting and Guiot's uses millimeters while three-dimensional MRIs are measured in voxels. Vim locations based on automatic indirect methods are compared with those based on manual determinations of neurosurgeons, and the results show similar positions between them. The similar positions prove Vim determination accuracy of proposed automatic indirect methods.

Left and right Vim locations are determined based on AC-PC planes. AC-PC planes are determined based on AC-PC points. If the AC-PC points are not aligned accurately, then AC-PC planes contain errors. The possibility of the occurrence of these errors is a cause of this paper to observe indirect methods not only in MRIs with the correct orientation of AC-PC planes but also those with the incorrect orientation of AC-PC planes. Based on the experiment conducted in this paper, Vim locations obtained by Guiot's are more accurate than those by Coordinate-based targeting in MRIs with the correct orientation of AC-PC planes. Guiot's has 0.05 mm smaller value of average error results than Coordinate-based targeting. In contrast, Vim locations based on Coordinate-based targeting are more accurate in the MRIs with the incorrect orientation of AC-PC planes. In summary, Guiot's provides more accurate Vim localization in MRIs with the correct orientation of AC-PC planes. Coordinate-based targeting has 0.032 mm smaller value of average error results than Guiot's. Nevertheless, Coordinate-based targeting method is more resilient with inaccuracy AC-PC planes.

The determination of AC-PC points is still manual in this study. Segmentation of AC and PC to automate the location of AC-PC points is the development of the continuation of this study.

Abbreviations

AC: Anterior Commissure; CC: Corpus Callosum; CT: Computerized Tractography; IPS: Inomed Planning Software; MR: Midline Reference; MRI: Magnetic Resonance Imaging; PC: Posterior Commissure; PD: Parkinson's disease; Vim: Ventral Intermediate Nucleus.

Availability of data and materials

The used raw dataset in this research is not publicly available. Readers can contact the author if they want to access the data

Competing interest

The authors declare that they have no competing interests.

Funding

This research did not receive any specific grant from funding agencies in the public, commercial, or not-for-profit sectors.

Authors' contributions

RS is the supervision that has the idea for creating automatic Vim localization. KRS composed the manuscript and did the experiment. MAR built the program. AF is neurosurgeon that operated on patients with Parkinson's disease and determine the used methods. AT and AHB are neurosurgeon that evaluates the results that are obtained by KRS. All authors read and approved the final manuscript.

Acknowledgements

Authors give a deep thank to National Hospital Surabaya and Dr. Soetomo General Academic Hospital that provides the MRIs of Parkinson's patients. This research was funded by the Indonesian Ministry of Education and Culture, and the Indonesian Ministry of Research and Technology/National Agency for Research and Innovation under RISPRO Invitation program managed by LPDP, under PPKI program managed by Institut Teknologi Sepuluh Nopember, and under World Class University Program managed by Institut Teknologi Bandung.

REFERENCES

1. Ray Dorsey E, Elbaz A, Nichols E, et al (2018) Global, regional, and national burden of Parkinson's disease, 1990–2016: a systematic analysis for the Global Burden of Disease Study 2016. The Lancet Neurology 17:939–953. https://doi.org/10.1016/S1474-4422(18)30295-3
2. Sammartino F, Krishna V, King NKK, et al (2016) Tractography-Based Ventral Intermediate Nucleus Targeting: Novel Methodology and Intraoperative Validation. Movement Disorders 31:1217–1225. https://doi.org/10.1002/mds.26633
3. Taira T, Horisawa S, Takeda N, Ghate P (2018) Stereotactic Radiofrequency Lesioning for Movement Disorders. Progress in Neurological Surgery 33:107–119. https://doi.org/10.1159/000481079

4. Mao Q, Qin W, Zhang A, Ye N (2020) Recent advances in dopaminergic strategies for the treatment of Parkinson's disease. Acta Pharmacologica Sinica 1–12
5. Blosser JA, Podolsky E, Lee D (2020) L-DOPA-Induced Dyskinesia in a Genetic Drosophila Model of Parkinson's Disease. Experimental Neurobiology 29:273
6. Nikkhah G, Carvalho GA, Pinsker M (2013) Functional Neurosurgery in Parkinson's Disease: A Long Journey from Destruction Over Modulation Towards Restoration. In: Nikkhah G, Pinsker M (eds) Stereotactic and Functional Neurosurgery. Springer Vienna, Vienna, pp 5–11
7. Sidiropoulos C, Mubita L, Krstevska S, Schwalb JM (2015) Successful Vim targeting for mixed essential and parkinsonian tremor using intraoperative MRI. Journal of the neurological sciences 358:488–489. https://doi.org/10.1016/j.jns.2015.08.1553
8. Dormont D, Seidenwurm D, Galanaud D, et al (2010) Neuroimaging and Deep Brain Stimulation. American Journal of Neuroradiology 31:15–23. https://doi.org/10.3174/ajnr.A1644
9. Diaz A, Cajigas I, Cordeiro JG, et al (2020) Individualized Anatomy-Based Targeting for VIM-cZI DBS in Essential Tremor. World Neurosurgery
10. Dembek TA, Petry-Schmelzer JN, Reker P, et al (2020) PSA and VIM DBS efficiency in essential tremor depends on distance to the dentatorubrothalamic tract. NeuroImage: Clinical 102235
11. Tani N, Morigaki R, Kaji R, Goto S (2014) Current Use of Thalamic Vim Stimulation in Treating Parkinson's Disease. A Synopsis of Parkinson's Disease 11:193
12. Milosevic L, Kalia SK, Hodaie M, et al (2018) Physiological mechanisms of thalamic ventral intermediate nucleus stimulation for tremor suppression. Brain 141:2142–2155. https://doi.org/10.1093/brain/awy139
13. Jakab A, Blanc R, Berényi EL, Székely G (2012) Generation of individualized thalamus target maps by using statistical shape models and thalamocortical tractography. American Journal of Neuroradiology 33:2110–2116. https://doi.org/10.3174/ajnr.A3140
14. Khaled M. Krisht, Mohammad Sorour, Martin Cote, et al (2015) Marching beyond the sella: Gerard Guiot and his contributions to neurosurgery. Journal of Neurosurgery 122:464–472. https://doi.org/10.3171/2014.10.JNS131919
15. Guiot G, Arfel G, Derome P, Kahn A (1968) [Neurophysiologic control procedures for sterotaxic thalamotomy]. Neuro-Chirurgie 14:553–566
16. Jakobs M, Krasniqi E, Kloß M, et al (2018) Intraoperative stereotactic MRI for deep brain stimulation electrode planning in patients with movement disorders. World Neurosurgery 1–8. https://doi.org/10.1016/j.wneu.2018.07.270
17. Hashizume A, Akimitsu T, Iida K, et al (2016) Novel software for performing leksell stereotactic surgery without the use of printing films: Technical note. Neurologia Medico-Chirurgica 56:193–197. https://doi.org/10.2176/nmc.tn.2015-0155
18. Tamura M, Hayashi M, Konishi Y, et al (2013) Advanced Image Coregistration within the Leksell Workstation for the Planning of Glioma Surgery: Initial Experience. Journal of Neurological Surgery Reports 74:118–122. https://doi.org/10.1055/s-0033-1358380
19. Fahmi A, Subianto H, Suroto NS, et al (2020) Stereotactic aspiration of spontaneous intracerebral hematoma: Case series. International Journal of Surgery Case Reports 72:229–232. https://doi.org/10.1016/j.ijscr.2020.06.008
20. inomed Medizintechnik Inomed Planning Software - IPS. https://www.en.inomed.com/products/functional-neurosurgery/ips/
21. Houshmand L, Cummings KS, Chou KL, Patil PG (2014) Evaluating indirect subthalamic nucleus targeting with validated 3-tesla magnetic resonance imaging. Stereotactic and functional

neurosurgery 92:337–345
22. Najdenovska E, Tuleasca C, Jorge J, et al (2019) Comparison of MRI-based automated segmentation methods and functional neurosurgery targeting with direct visualization of the Ventro-intermediate thalamic nucleus at 7T. Scientific Reports 9:1–13. https://doi.org/10.1038/s41598-018-37825-8
23. Eisinger RS, Wong J, Almeida L, et al (2017) Ventral Intermediate Nucleus Versus Zona Incerta Region Deep Brain Stimulation in Essential Tremor. Movement Disorders Clinical Practice 5:75–82. https://doi.org/10.1002/mdc3.12565
24. Bazin P, Sciences B, Gandler W, et al (2005) Free software tools for atlas-based volumetric neuroimage analysis Free Software Tools for Atlas-based Volumetric Neuroimage Analysis. https://doi.org/10.1117/12.595602
25. Weiss KL, Pan H, Storrs J, et al (2003) Clinical brain MR imaging prescriptions in Talairach space: technologist-and computer-driven methods. American journal of neuroradiology 24:922–929
26. Bar-Itzhack IY (2000) New method for extracting the quaternion from a rotation matrix. AIAA Journal of Guidance, Control and Dynamics 23:1085–1087
27. Cariow A, Cariowa G, Majorkowska-Mech D (2020) An Algorithm for Quaternion-Based 3D Rotation. International Journal of Applied Mathematics and Computer Science 30:149–160. https://doi.org/10.34768/amcs-2020-0012
28. Rivera JDDS (2020) Training an image classifier with transfer learning on Node. js. In: Practical TensorFlow. js. Springer, pp 185–201

Figures

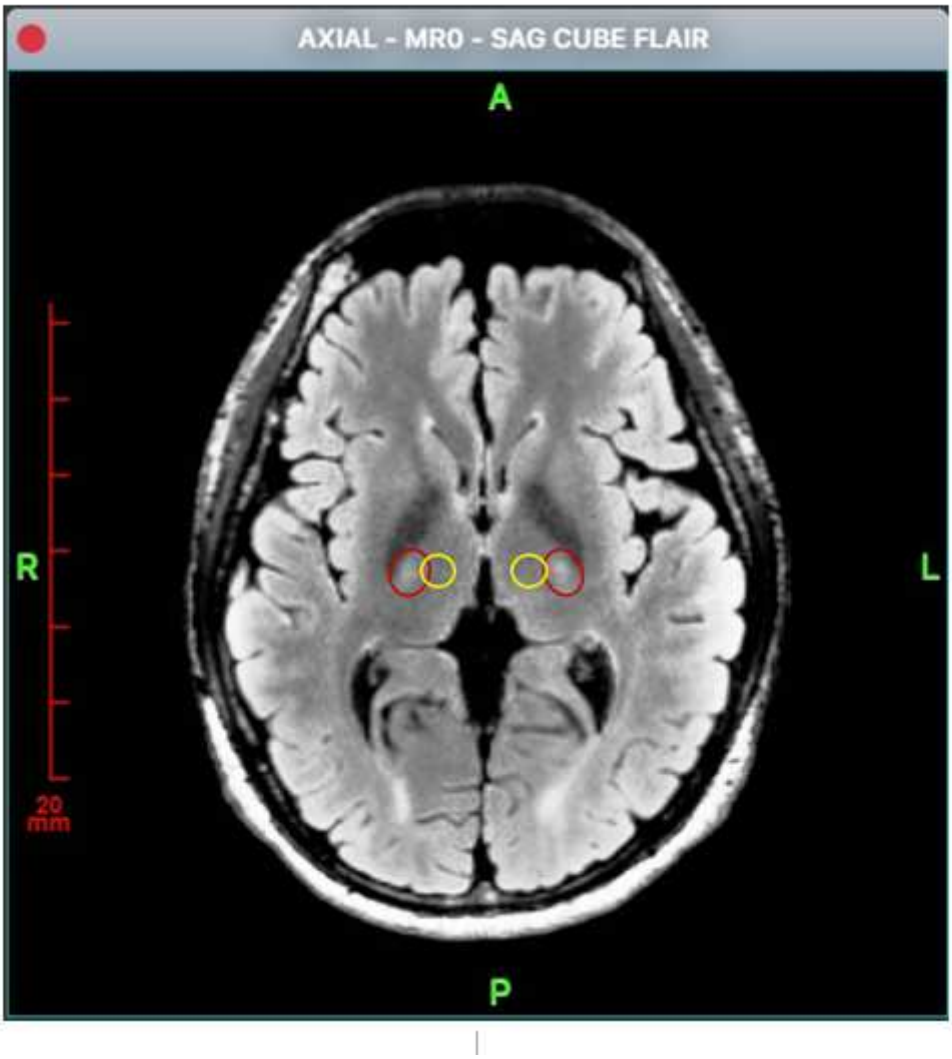

Figure 1

Axial plane in 3T brain magnetic resonance imaging (MRI)

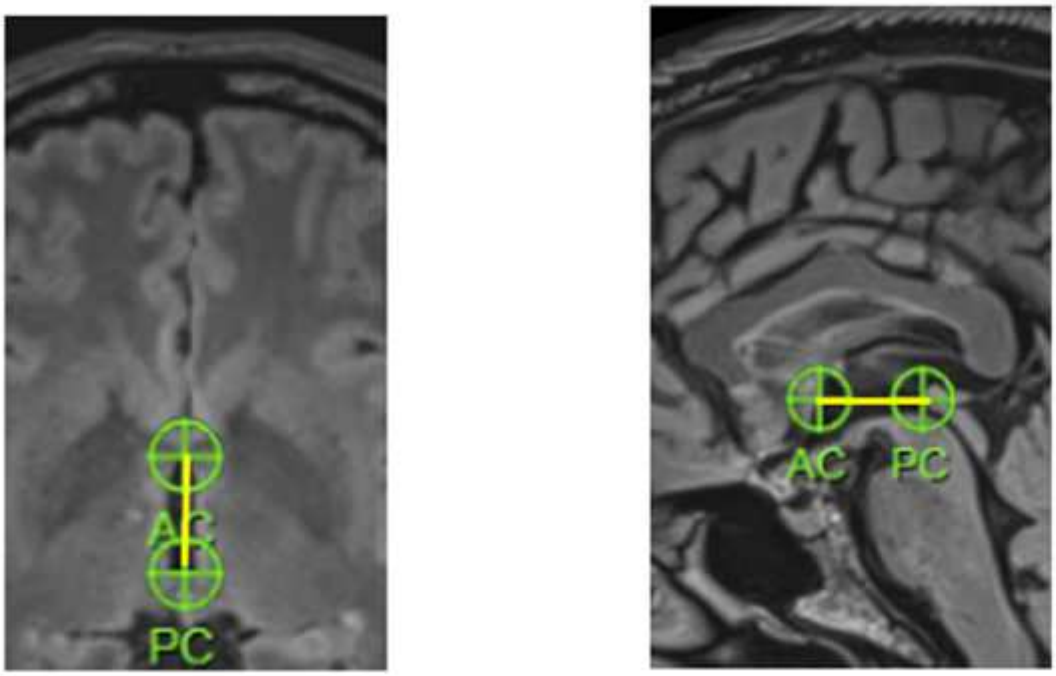

(a) Axial plane (b) Sagittal plane

Figure 2

AC-PC in the axial plane and the sagittal plane

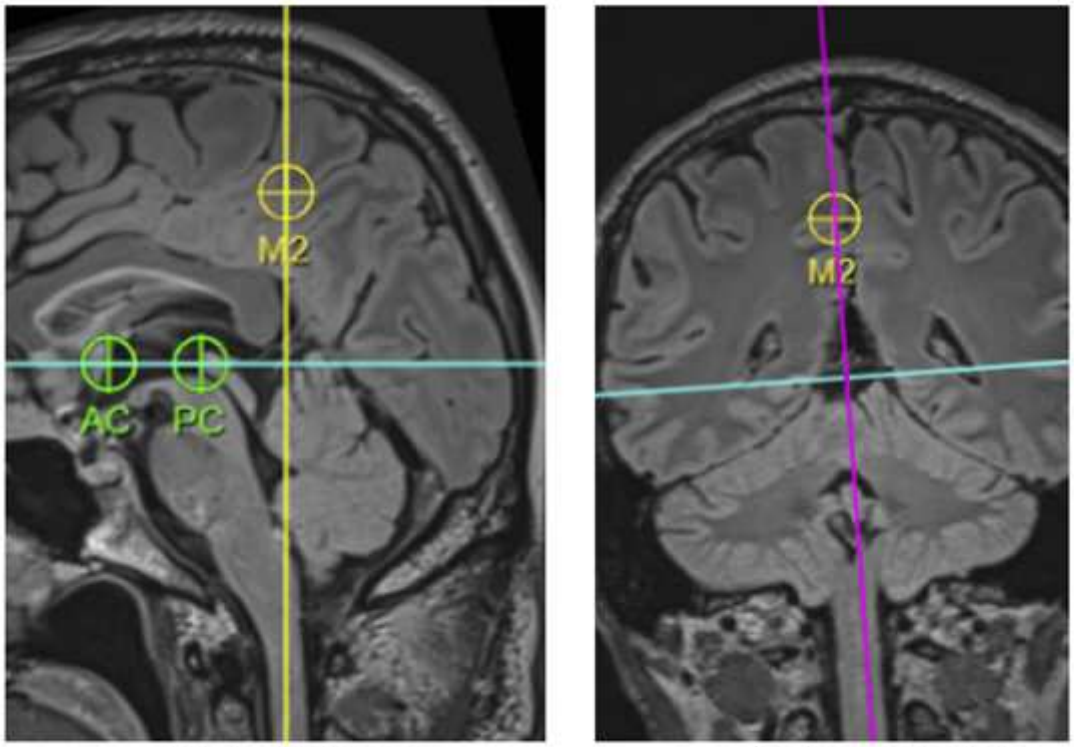

(b) Sagittal plane (b) Coronal plane

Figure 3

MR in the sagittal plane and the coronal plane

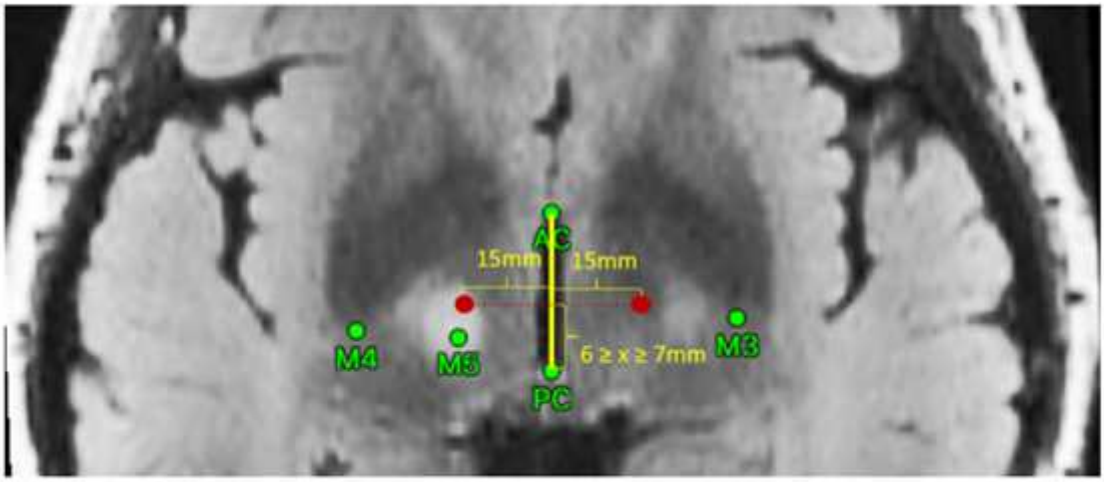

Figure 4

Coordinate-based targeting method

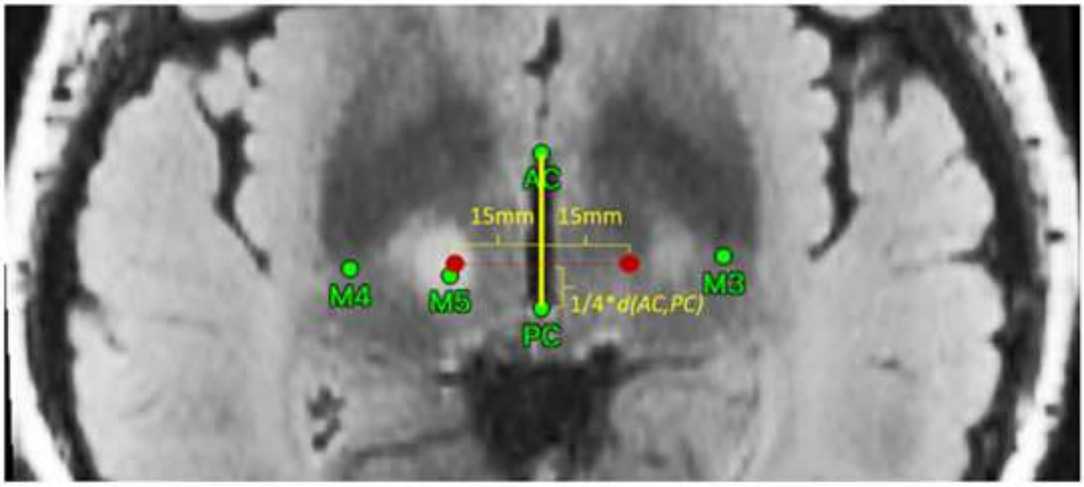

Figure 5

Guiot's method

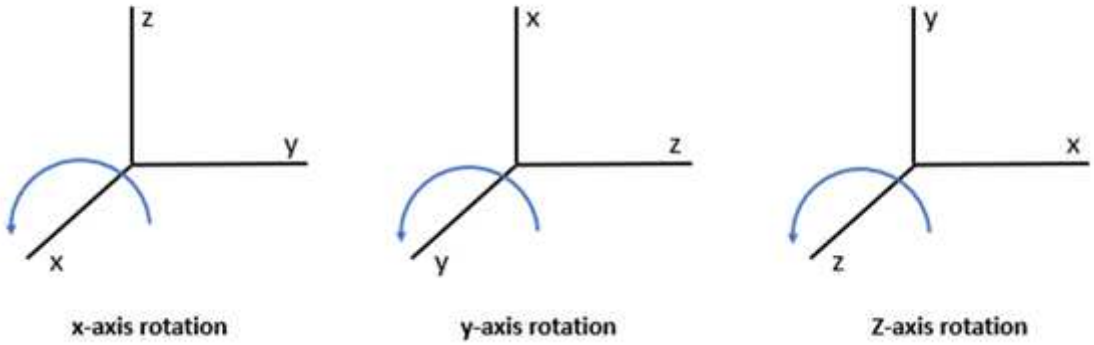

Figure 6

3D Axis Rotation

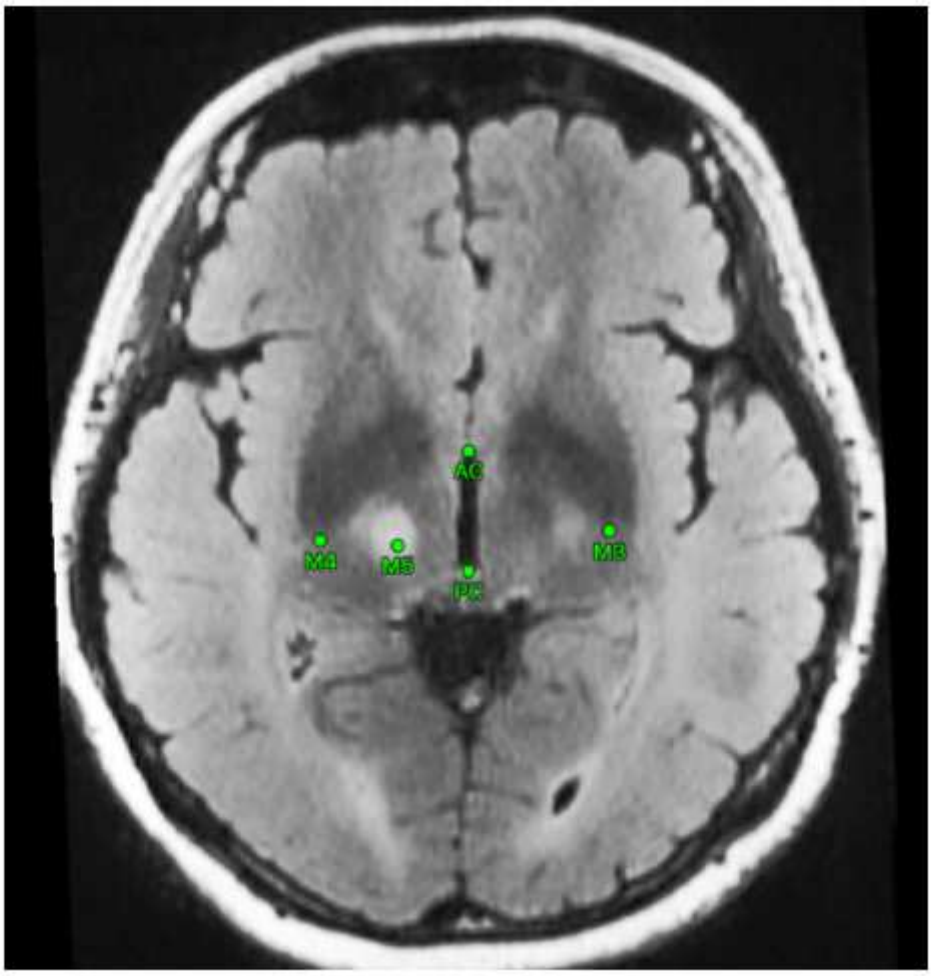

Figure 7

Axial plane of post-operative T2-Flair Brain MRI

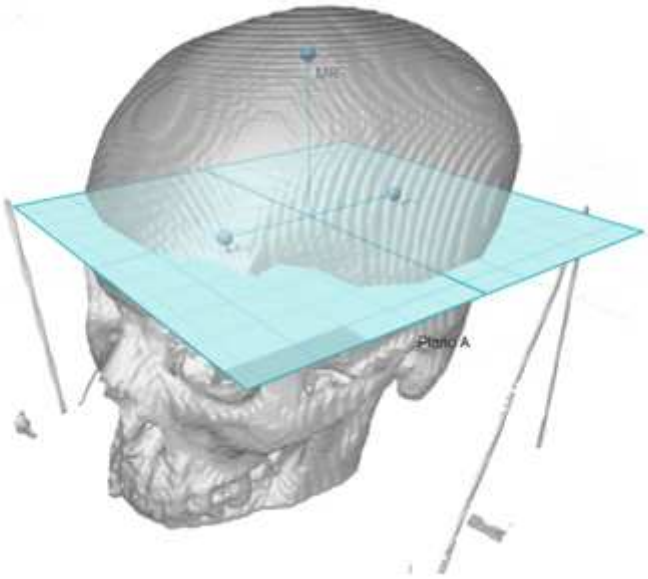

Figure 8

Visualization of a plane that is inside a head

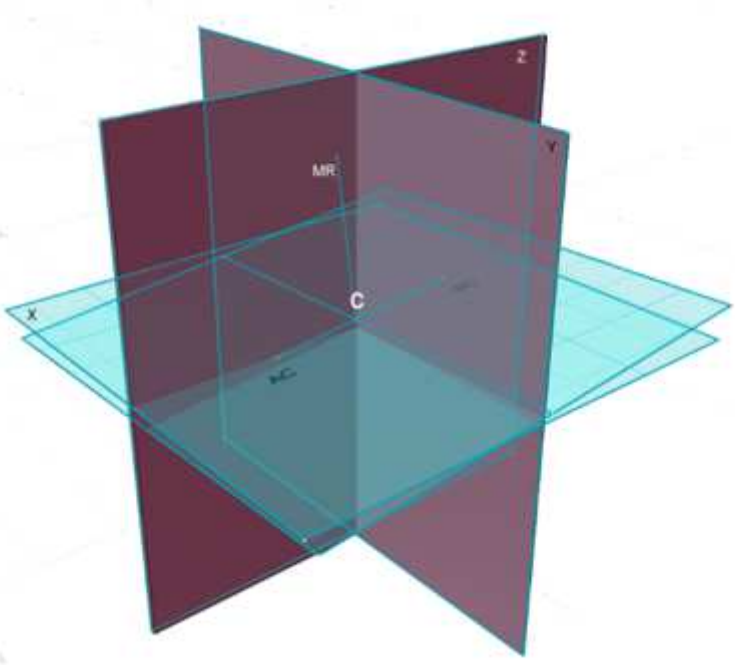

Figure 9

The position of Plane A between normal x-plane, y-plane, and z-plane.

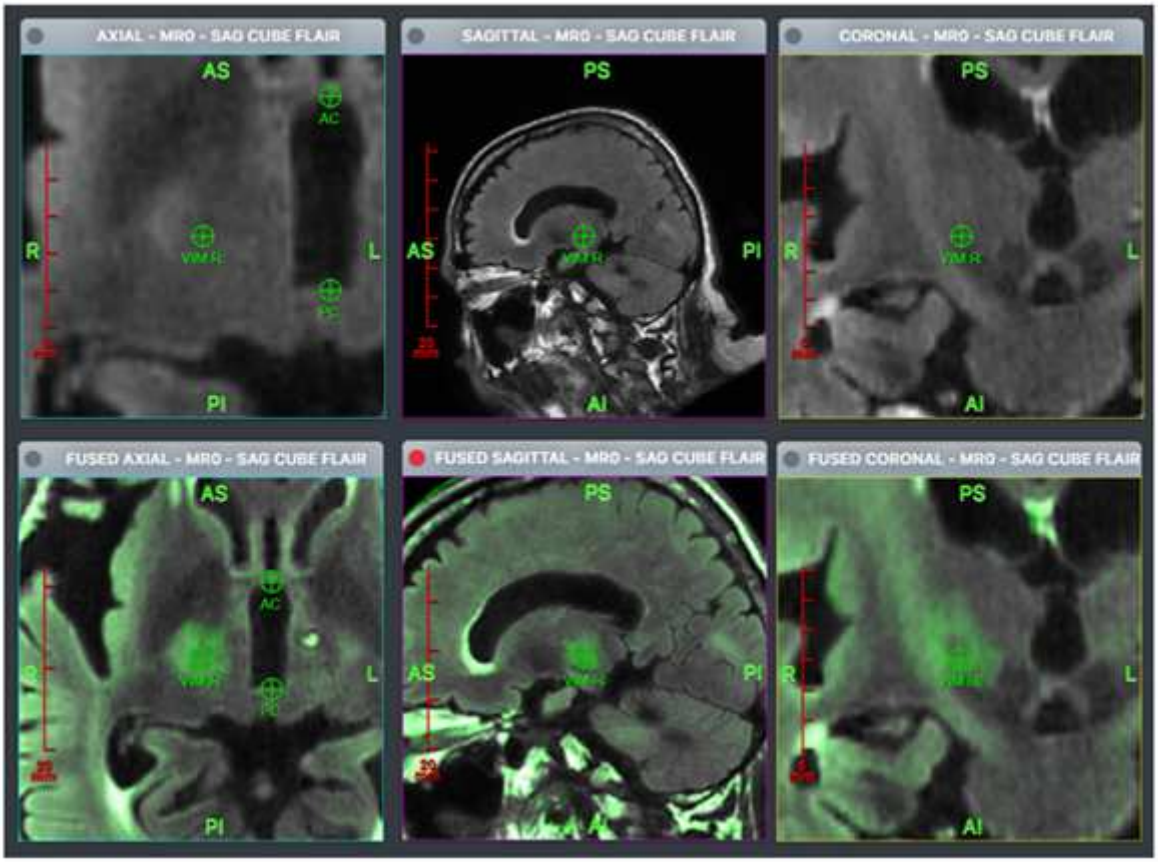

Figure 10

Comparison between the proposed method (above) and the manual determination of a neurosurgeon (below).

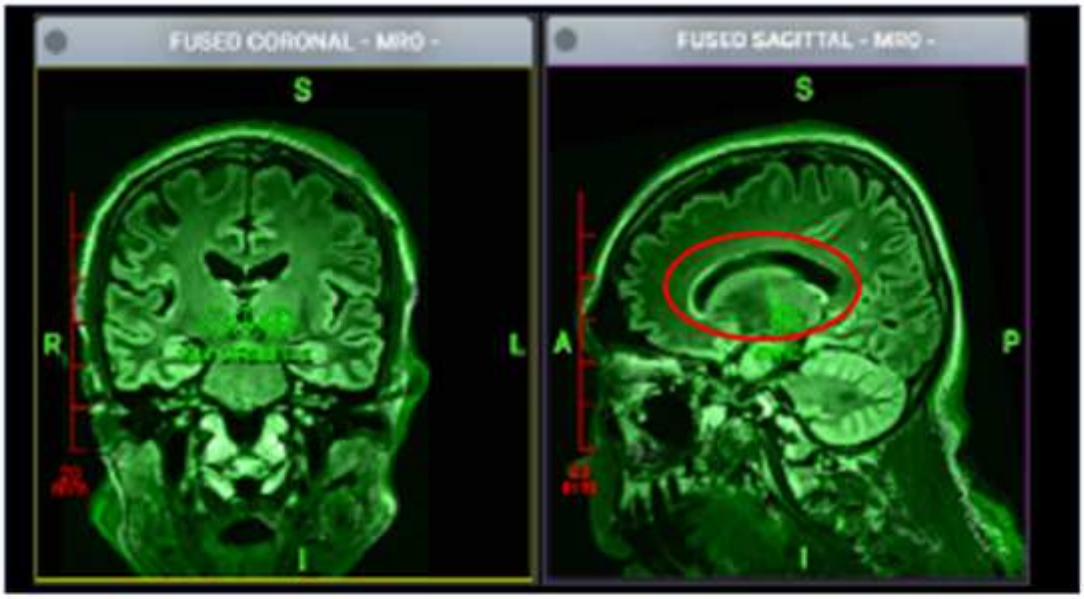

(a) Coronal and Axial Planes of a person with Parkinson's Disease without Having Cyst

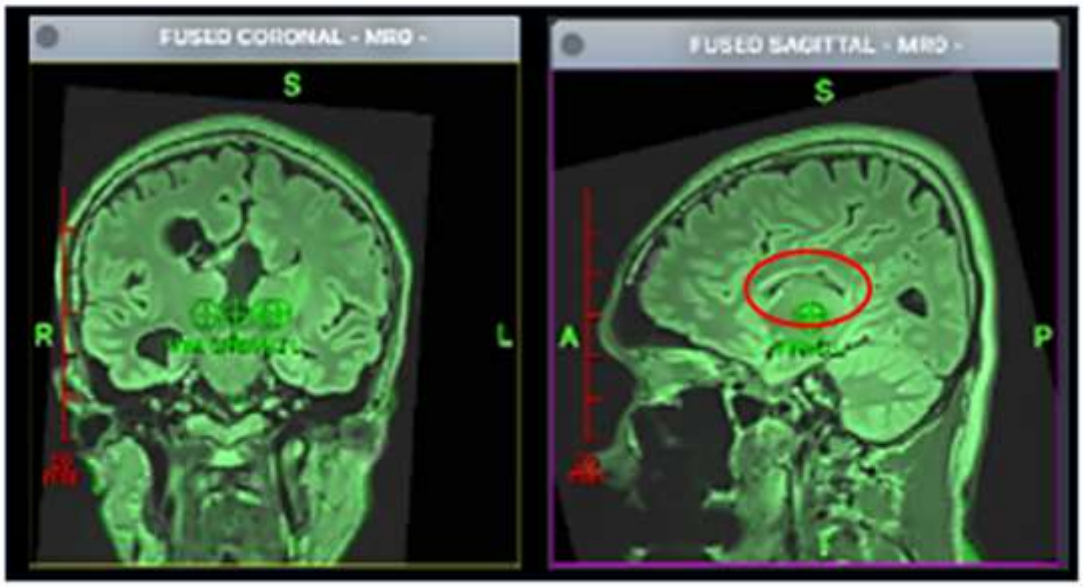

(b) Coronal and Axial Planes of a person with Parkinson's Disease with Having Cyst

Figure 11

Comparison of MRIs with and without Cyst